

# A Frequency Method for Fatigue Life Estimation of Mechanical Components under Bimodal Random Stress Process

C. Braccesi<sup>1</sup>, F. Cianetti<sup>1</sup>, G. Lori<sup>1</sup> and D. Pioli<sup>1</sup>

**Abstract:** This paper describes an original frequency method for fatigue life estimation of mechanical components subjected to random inputs. Currently mechanical components life design under random loads is an important task of the research, due to the increasing importance of virtual simulation in opposition to the experimental tests. The frequency domain approach, in this context, seems to be able to supply reliable estimations with small computational effort. The proposed method belongs to the class of corrective coefficient to narrow-band formula methods and it has been thought for bimodal *PSDs*. The definition of the generalized bimodal processes and the research of the links between corrective coefficient and the system dynamic behaviour are other original aspects of this work.

**keyword:** Fatigue life, Frequency domain approach, Bimodal *PSD*.

## 1 Context

Fatigue life estimation of mechanical components subjected to random loads is an important topic of machine design. For this reason in the last years the scientists are trying to supply optimized instruments to this field of the planning. The interest is particularly directed on the virtual simulation of the operative conditions: the computational performance increasing and the requirement to minimize costs are the principal causes of this fact. Research on virtual damage evaluation is object of authors activity [Braccesi, Cianetti, Lori and Pioli (2005)] and this paper is centred on a particular problem of this procedure, that is the frequency damage estimation starting from *Power Spectral Density (PSD)* of stress random processes. Fig. 1 illustrates the general flow-chart of vibration fatigue. As example of application the authors had chosen a car chassy excited by the roughness of road surface [Braccesi, Cianetti and Landi (2005)]. A finite ele-

ment (FE) model of the chassis has been created and then it has been assembled (by modal synthesis) in a multi-body simulation (MBS) environment together with the principal components of the car. The results of dynamic analysis on this model have been used by the authors to make a detailed study of some aspects not yet solved. As shown in Fig. 1 there are two possible approach for the virtual simulation of mechanical components [Braccesi, Cianetti, Lori and Pioli (2004)]. The first is the time-domain approach and it is the reference method because it supplies reliable results (but with large computational times). In fact the central part of this procedure is the transient analysis which becomes very heavy with the increase of the degrees of freedom (dof) number. The frequency domain analysis can solve this problem by system linearization and frequency response calculation and it allows to have frequency representation of stress state in reduced times. From these inputs a frequency method evaluates fatigue damage much more quickly than the Rainflow counting in the time-domain. A special class of frequency methods [Wirsching and Light (1980), Lutes (1990)] corrects damage estimation of a simple theory named narrow-band formula [Bendat (1964)]. The corrective coefficient dependence by stress *PSD* parameters is an interesting aspect that usually in literature has been studied only by the analytical side. Instead the authors want to show as this coefficient is strictly related to the dynamical behaviour of the mechanical component and the definition of coefficient as a system property is a future objective of the research. Moreover many other fields of research are open, that are not object of this paper. In fact, as it can be seen in Fig. 1, generally the system has not a linear behaviour, so another corrective coefficient depending on normality indexes of stress output process can be evaluated [Kihl, Sarkani and Beach (1995)]. However, multiaxiality is certainly the greatest question to solve: in this work a preliminary hypothesis consists in considering a uniaxial state of stress, but usually the stress state is biaxial or triaxial. In literature there are many multiaxial criteria [You and Lee

<sup>1</sup> University of Perugia, Perugia, Italy. Extended English version of the paper presented at XXXIV AIAS Conference

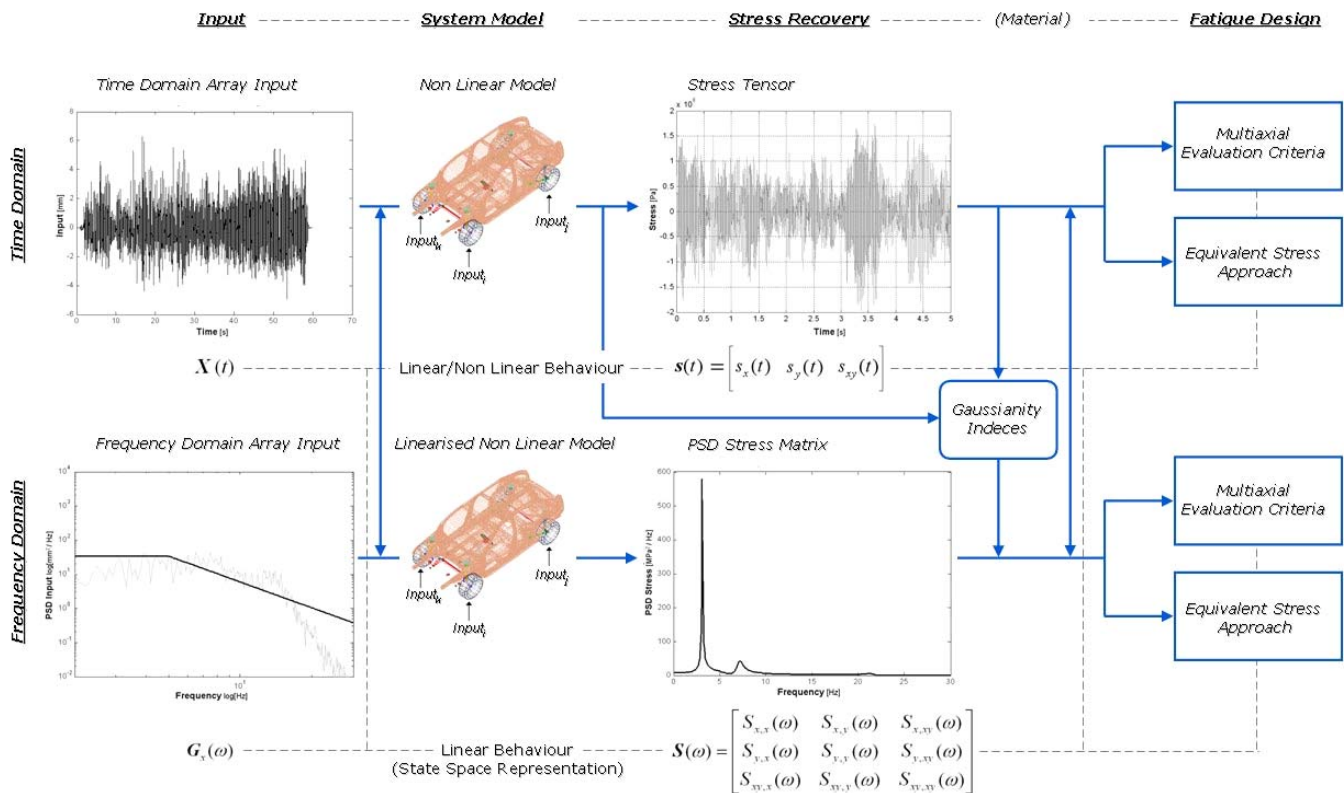


Figure 1 : Flow-chart of the vibration fatigue evaluation processes

(1996)], but the authors believe that the equivalent uniaxial stress is the method more adaptable to frequency domain approach [Braccesi, Cianetti, Lori and Pioli (2005), Pitoiset, Rychlik and Preumont (2001)]. The definition of an equivalent uniaxial stress makes the theory of the present paper general.

**2 Frequency methods. Narrow-band formula. Bimodal PSD.**

A frequency direct method consist in an analytical formulation for the damage evaluation starting from frequency representation of stress conditions [Bishop (1988)], that is the Power Spectral Density of the random scalar process if mechanical components stress conditions are roughly uniaxial. Under these stress conditions the time-domain procedure firstly factorizes stress history by a counting method (usually in the Rainflow Cycle Counting method [Matsuishi and Endo (1968)]), then utilizes Wohler’s curve and Miner’s linear cumula-

tion rule. About the translation of this approach in frequency domain a very hard problem has to be solved, because counting method was created by researchers in order to work in the time-domain, therefore some steps of the counting algorithm are transferable on frequency only by complications that are incompatible with design duration [Bishop and Sherratt (1990)].

Depending on this lack of a general theory, some frequency methods are based on a correction factor of the damage of a special class of random process: the narrow-band process [Bendat (1964)]. In the time domain this can be seen as a sinusoidal signal with constant period and continuously variable amplitude (see Fig. 2). In the same way a typical frequency representation, which is illustrated in Fig. 3, shows a function concentrated around a central frequency. A fundamental theoretical conclusion about the narrow-band Gaussian process indicated that its probability density function (pdf) of extremes is a

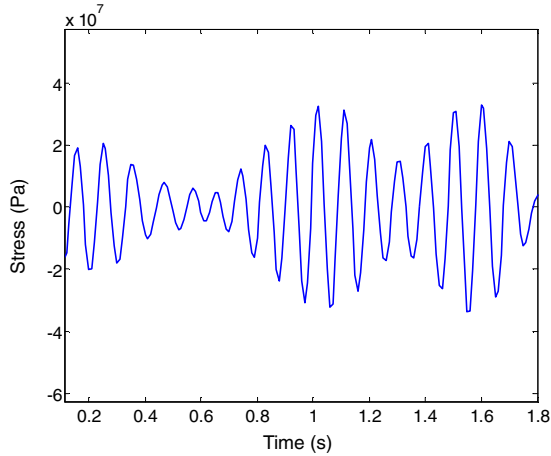


Figure 2 : Narrow-band stress time history

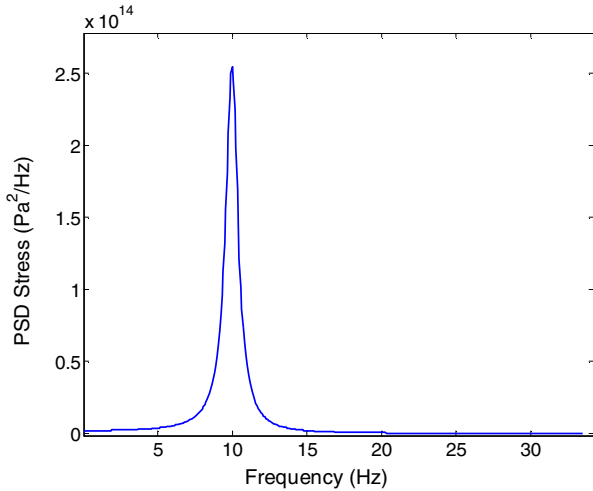


Figure 3 : PSD of narrow-band stress process

Rayleigh distribution (see Fig. 4)[Rice and Beer (1965)]:

$$P_{NB}(s) = \frac{s}{4M_0} e^{-\frac{s^2}{8M_0}} \quad (1)$$

In Eq. (1)  $s$  represents two times of the level of extreme stress and  $M_0$  is the order zero spectral moment of stress one-sided PSD, named by  $S(f)$ . A  $n$ -order spectral moment of PSD is defined by [Vanmarke (1972)]:

$$M_n = \int S(f) f^n df \quad (2)$$

It is easy to understand that  $M_0$  is equal to the area subtended by PSD. It means that is possible to evaluate fatigue damage by a simple integration: in fact for a narrow-band time-history it is obvious that each peak

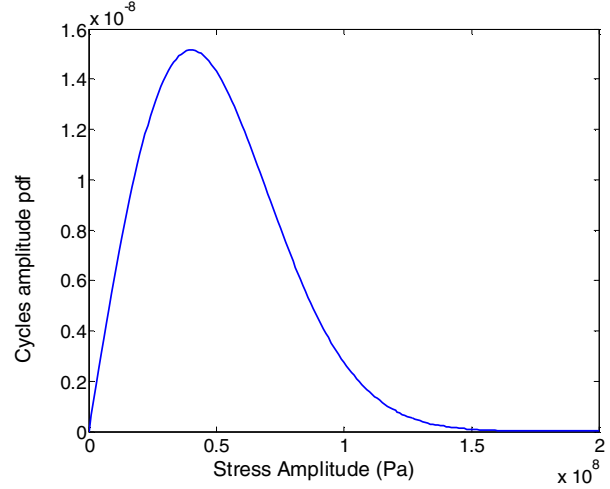


Figure 4 : Rayleigh's cycles amplitude pdf for the process of Fig. 2 and Fig. 3

is followed by a valley characterized by the same magnitude. The *Rainflow Cycle Counting* couples just these extremes to forming an elementary fatigue cycle: therefore  $P_{NB}(s)$  is also the probability density function of the fatigue cycles range (the range is twice of the amplitude) and the damage expected value can be calculated introducing in the general formulation of the following Eq.3 the expression for  $P(s)$  described by Eq. 1. The fatigue strength curve of material is expressed by the law  $Ns^m = k$ .

$$E[D] = \frac{\nu_P T}{k} \int s^m P(s) ds \quad (3)$$

In the previous equation  $T$  symbolizes stress time history duration, while  $\nu_P$  (the peaks rate) can be evaluated by the following relation [Vanmarke (1972)]:

$$\nu_P = \sqrt{\frac{M_4}{M_2}} \quad (4)$$

However the narrow-band theory can be utilized only in a few practical applications. For example a simple test case is shown in Fig. 5: even for a clamped-clamped beam in the stress response PSD two spectral area peaks appear. In fact the shape of stress random process is depending on the number and the features of dynamical system resonances which have been excited by the input. Therefore it can be understood that the bimodal PSD, represented in Fig. 6 (both in time domain and in frequency domain), is more interesting rather than unimodal (narrow-band) PSD.

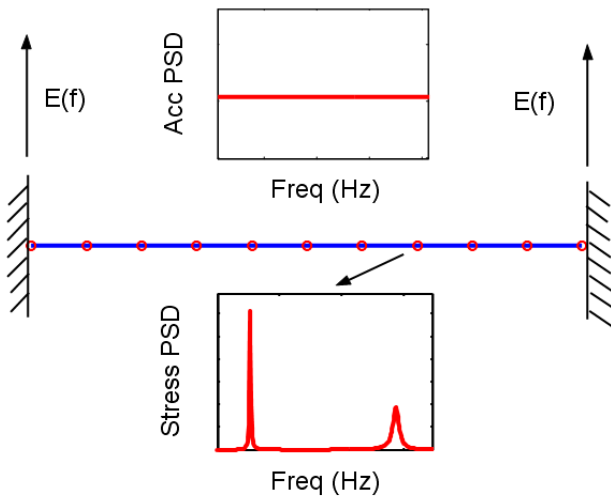


**Figure 5 :** Dynamical excitation of clamped-clamped beam

An important class of frequency methods is based on a corrective coefficient applied to the narrow-band formula [Wirching and Light (1980), Lutes 1990)]. This corrective coefficient, named  $\lambda$  frequently in literature, is a function of the stress PSD spectral moments and it can be showed that always it is less than one. Therefore it can be written:

$$D = \lambda D_{NB} \tag{5}$$

As previously explained  $D_{NB}$  can be evaluated by:

$$D_{NB} = \frac{v_{PT}}{k} \int s^m P_{NB}(s) ds \tag{6}$$

In a corrective coefficient frequency method the greatest problem is related to the analytical model parameter optimization. This model obviously has to converge to unity when the stress random process approaches narrow-band situation. On the contrary  $\lambda$  aims to zero as much as the process contains a frequency wide band. A fundamental parameter which is able to reproduce this behaviour is the irregularity factor  $\gamma$  [Vanmarke (1972)]:

$$\gamma = \frac{M_2}{\sqrt{M_0 M_4}} \tag{7}$$

The interpretation of Eq. 7 can be made easier remembering Eq. 4 and also introducing the following time-frequency relation for the mean (zero) value upcrossings

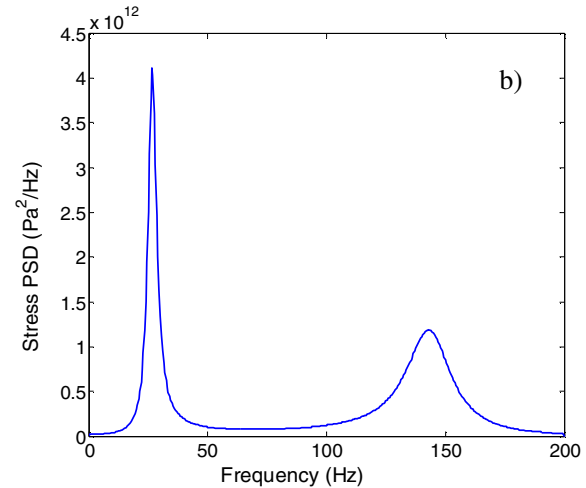
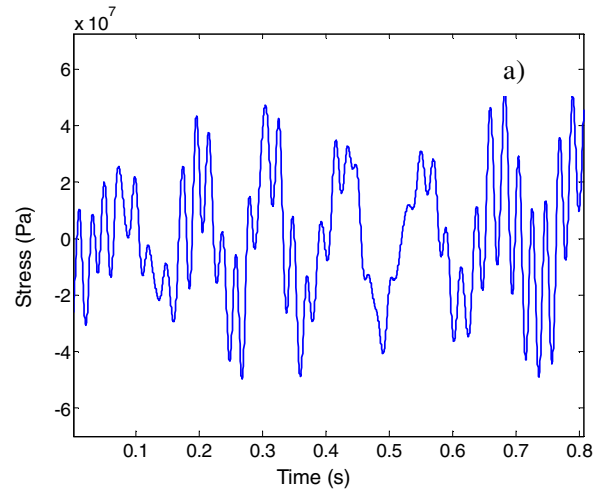


**Figure 6 :** Bimodal random process in time-domain (a) and in frequency-domain (b)

rate:

$$v_0 = \sqrt{\frac{M_2}{M_0}} \tag{8}$$

It can be easily observed that irregularity factor is coincident to the ratio between upcrossings rate  $v_{-0}$  and peaks rate  $v_{-p}$ . When the time signal is strictly narrow-band this ratio is close to unity, while it goes to zero as much as the process is wide-band. Therefore for the analytical model definition of corrective coefficient it is possible to take advantage by its inverse proportion to  $\gamma$ . Moreover it will be seen later that the irregularity factor can be simply expressed by other PSD bimodal parameters that have an immediate geometrical interpretation. In the following paragraph it will be shown as the authors have created [Braccesi, Cianetti, Lori and Pioli (2004)] a new model

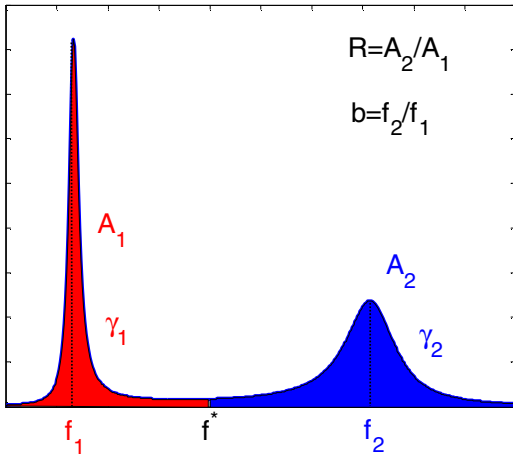


Figure 7 : Geometrical parameters of bimodal PSD

of corrective coefficient based on these few geometrical parameters, represented in Fig. 7. Essentially the spectral area is divided into two zone: one is under the influence of the first peak, the other belong to the second peak. In this manner it is possible to lead the bimodal PSD to the interaction between two unimodal processes. Areas, central frequencies and irregularity factors of single unimodal processes will form the variables set of the model. In literature many researchers [Lutes and Sarkani (1997)] prefer to utilize this set of parameters into damage analytical model because it is more flexible than PSD spectral moments and especially it is more useful during the optimization of the analytical functions coefficients.

### 3 IEP method

This part of the paper presents an original frequency method proposed by the authors and based on a simple model for the corrective coefficient to the narrow-band formula. In this paragraph the authors try to explain the reasons driving them in research activity. Firstly this original formulation is explained, emphasizing its theoretical basis and showing the good agreement that it supplies by the comparison with data coming from simulated time histories. Then an extension of classical definition of bimodal PSDs will be presented, enlarging the applicability field of the proposed method. Finally, it will be shown that the choice of the model independent variables is strictly related to the dynamic behaviour of the mechanical component.

The main objective of this activity consists in the explic-

itation of  $\lambda$  coefficient dependence on a suitable parameters set of bimodal process. Initially this functional relation can be written as:

$$\lambda = \lambda(A_1, A_2, f_1, f_2, \gamma_1, \gamma_2, k, m) \quad (9)$$

Where  $k$  and  $m$  are the Wohler's curve coefficient, while with reference to Fig. 7 the spectral parameters can be defined as follows:

$$A_1 = \int_0^{f^*} S(f)df \quad A_2 = \int_{f^*}^{f_{\max}} S(f)df \quad R = \frac{A_2}{A_1} \quad (10)$$

$$f_1 = \frac{\int_0^{f^*} S(f)fd f}{A_1} \quad f_2 = \frac{\int_{f^*}^{f_{\max}} S(f)fd f}{A_2} \quad b = \frac{f_2}{f_1} \quad (11)$$

$$\gamma_1 = \frac{\int_0^{f^*} S(f)f^2df}{\sqrt{A_1 \int_0^{f^*} S(f)f^4df}} \quad \gamma_2 = \frac{\int_{f^*}^{f_{\max}} S(f)f^2df}{\sqrt{A_2 \int_{f^*}^{f_{\max}} S(f)f^4df}} \quad (12)$$

Eq. 9 involves an high number of variables, but later on it will be indicated how to reduce the problem complexity; everyone of these variable can be associated to one of the determinant factor of this phenomenon that are material fatigue behaviour, level of the input and system dynamic properties. Therefore it can be interesting to separate these different effects into  $\lambda$  analytical formulation. Fig. 8 shows very well this concept.

#### 3.1 Triangular PSD

Bimodal processes are often reduced into geometrical elementary shape, especially when it is necessary to simulate many time histories from PSDs with much different parameters. Certainly the shape more utilized at this purpose is the rectangular shape: it has a reduced number of independent variables and it is suitable for a exact control of the simulation condition. However the authors have chosen the triangular shape (see Fig. 9), because it is as simple as the rectangular shape, and it approaches better the real behaviour of the dynamic resonances. About the use of triangular shape PSD for explicitation of expression in Eq. 9 is necessary to carry out some observations. Firstly in a previous publication [Braccesi, Cianetti, Lori and Pioli (2005)] the authors demonstrated that is not possible to value sensible variations of irregularity factors  $\gamma_1$  and  $\gamma_2$  by changing bandwidth of single triangular peaks. However this limitation is not a great difficulty, because the bandwidth factor of unimodal PSD

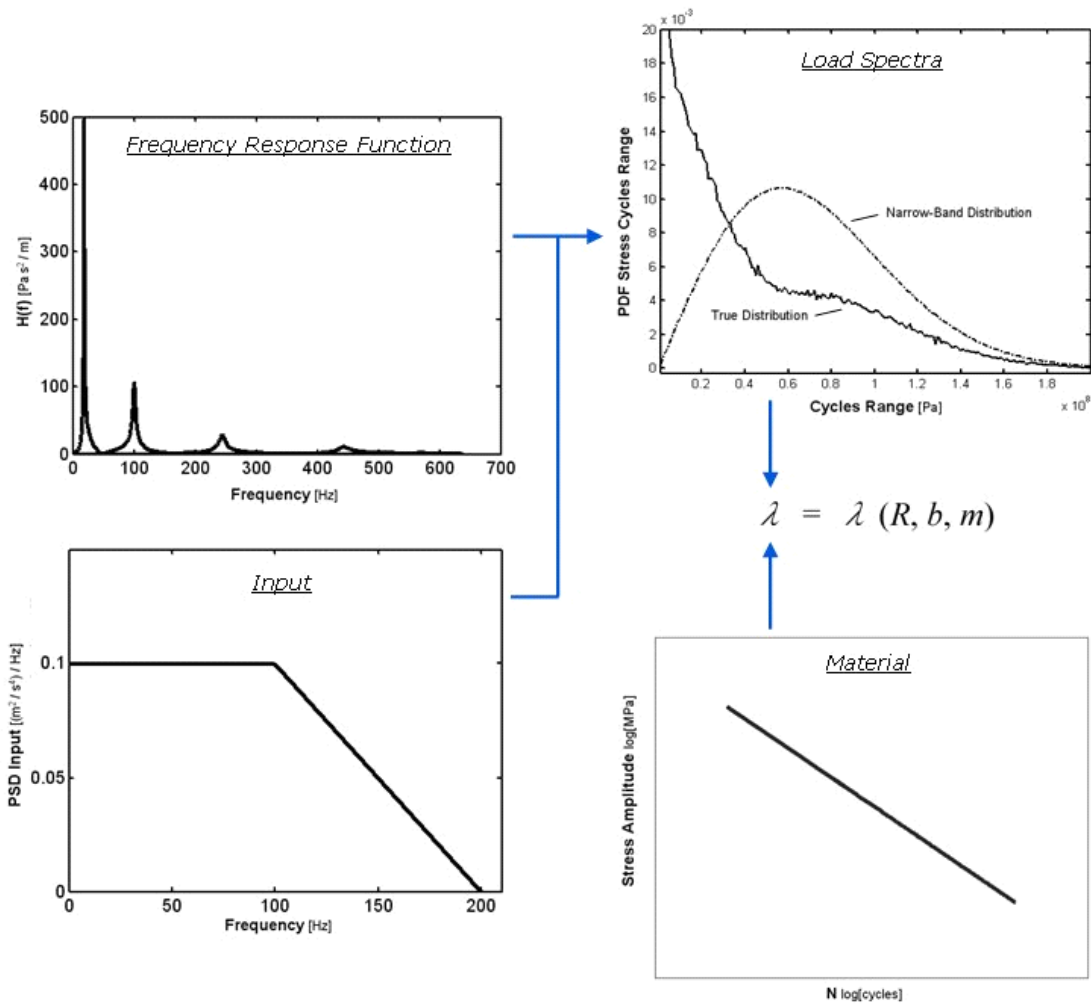


Figure 8 : Influence of principal factor on the corrective coefficient

component had a secondary influence respect to the ratio between their own central frequencies. An evidence of this property is in the good agreement between the irregularity factors of simulated time histories with different single peaks bandwidth and the values supplied by the rough formula (see Eq. 13), which can be obtained by the Eq. 14 for the spectral moments:

$$\lambda = \frac{1 + Rb^2}{\sqrt{(1 + R)(1 + Rb^4)}} \tag{13}$$

$$M_n = A_1 f_1^n + A_2 f_2^n \tag{14}$$

Another fact has been demonstrated in a previous paper of the authors: the dependence of  $\lambda$  by the central frequencies  $f_1$  and  $f_2$  is fully represented by their own ratio  $b$ .

On the base of this consideration the relation expressed by Eq. 9 can be simplified in following manner:

$$\lambda = \lambda(A_1, R, b, k, m) \tag{15}$$

### 3.2 Linear relation

From Eq. 5, remembering Eq. 3 and Eq. 6, it can be written:

$$\lambda = \frac{D}{D_{NB}} = 1 - \frac{D_{NB} - D}{D_{NB}} = 1 - \frac{\int s^m (P_{NB}(s) - P(s)) ds}{\int s^m P_{NB}(s) ds} \tag{16}$$

Eq. (16) can be also expressed as:

$$\lambda = 1 - \frac{A_1^{\frac{m}{2}}}{\int s^m P_{NB}(s) ds} IEP_m \tag{17}$$

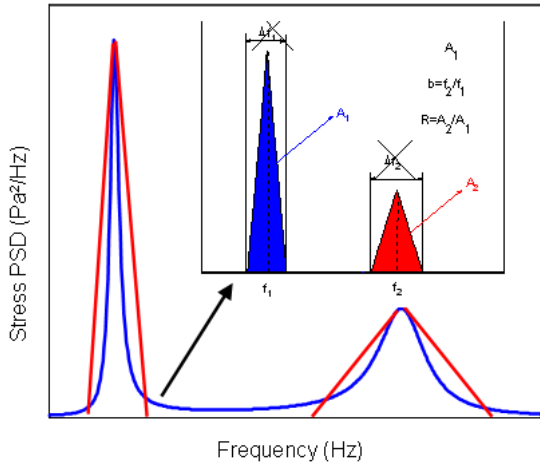


Figure 9 : Triangular shape of bimodal PSD

if the quantity named  $IEP_m$  assumes the form:

$$IEP_m = \frac{\int s^m (P_{NB}(s) - P(s)) ds}{A_1^{\frac{m}{2}}} \quad (18)$$

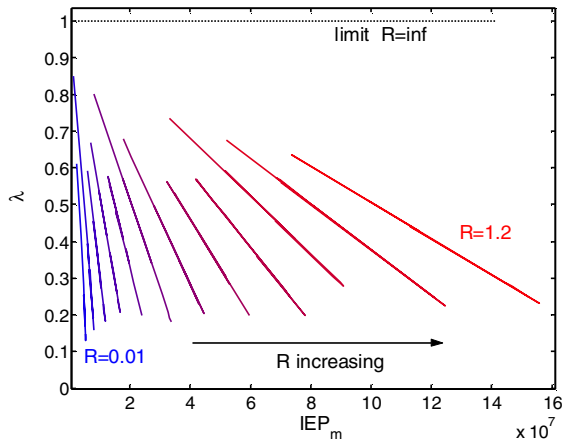


Figure 10 : Linear dependence between  $\lambda$  and  $IEP_m$

The multiplying factor  $IEP_m$  in Eq. 17 is a constant when  $A_1$  and  $R$  are fixed, therefore it is independent by  $b$ . Fig. 10 shows this linear dependence between the quantity  $IEP_m$ , which is related to the integrated difference  $P_{NB}(s) - P(s)$ , and the corrective coefficient for different values of  $R$  when  $m$  and  $A_1$  are fixed.

The original denomination  $IEP_m$  has been chosen by the authors [Braccesi, Cianetti, Lori and Pioli (2004)] because it represents a weighted difference of  $m$  order between the cycles range pdf of narrow-band formula and

the cycles range pdf of effective random process. ( $IEP$  is an acronym of Italian locution “Indice di Errore Pesato”). In the following paragraph it will be shown as it is possible to supply a meaning to this quantity, and as it can be expressed in dependence of the model variables.

### 3.3 First order IEP and m order IEP

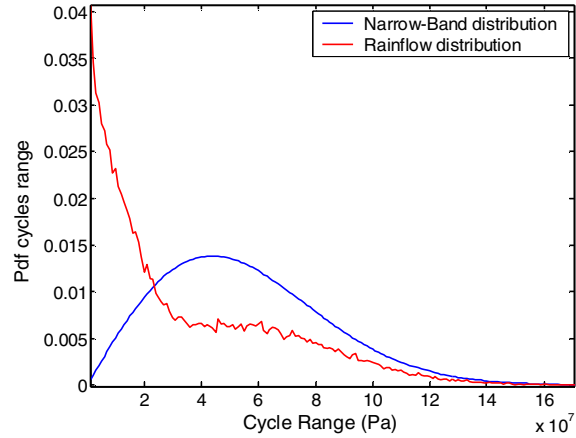


Figure 11 : Differences between narrow-band cycles range distributions evaluated from PSD and from a sample time history

Fig. 11 shows the difference between narrow-band cycles range distribution and the same distribution evaluated from a sample time history of a particular random bimodal PSD. The quantity  $IEP$  can be defined:

$$IEP = \frac{\int (P_{NB}(s) - P(s)) ds}{\sqrt{A_1}} \quad (19)$$

As previously stated the  $IEP_m$  index weights by the slope of Wohler’s curve the errors committed by the narrow-band theory applied in the wide-band situations.  $IEP$  also weights these errors, but in linear manner (see Fig. 12).

Discrete evaluation of the  $IEP$  starting from the distribution of fatigue cycles range calculated by a sample time history can be made changing the integral in Eq. 19 with a discrete sum:

$$IEP = \frac{\sum_{i=1}^{N_r} (P_{NB}(s_i) - P(s_i)) \Delta s}{\sqrt{A_1}} \quad (20)$$

$N_r$  is the number of range intervals utilized, each one of amplitude  $\Delta s$ .

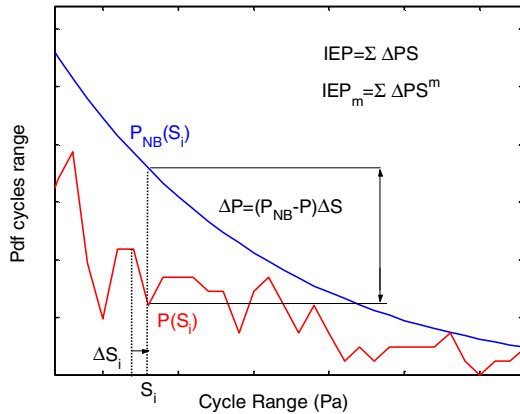


Figure 12 : Discrete evaluation of  $IEP$  and  $IEP_m$

The greater property of  $IEP$  consists in its independence by  $A_1$ . Therefore it is possible to express  $IEP$  by a function of  $R$  and  $b$ . The correct identification of this analytical constraint has been analyzed by the authors using extensive numerical simulations of sample time histories with different  $R$  and  $b$ . An accurate estimation in fact requires that the rainflow distribution has been fully converged. For this purpose results of 10 time histories with  $10^5$  fatigue cycles has been averaged, for each pair of  $R$  and  $b$  respectively varying in the ranges  $[0.01, 1.44]$  and  $[1.5, 10.5]$ .

The fitting operations of these results allow to evaluate for  $IEP$  the following analytical dependence:

$$IEP = \alpha(R) \exp\left(\beta(R)b^{\delta(R)}\right) \quad (21)$$

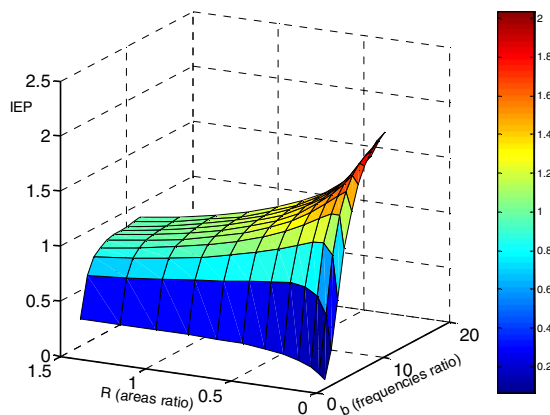


Figure 13 : Map of  $IEP$  vs.  $b$  and  $R$

The quantities  $\alpha$ ,  $\beta$  and  $\delta$  depend only by  $R$  and can be explicated by a polynomial function of third order with coefficients estimated through least squares approximation. In Fig. 13  $IEP$  values supplied by Eq. 21 are illustrated respect to  $R$  and  $b$ . Fig. 14 instead shows the normalized differences between same values of Fig. 13 and the original data estimated by sample time histories. Therefore these differences can be considered as the fitting errors related to the analytical modelling of simulated data.

A similar approach has been utilized for the fitting operations of  $IEP_m$ , under the hypotheses of its dependence on  $R$ ,  $m$  and  $IEP$ :

$$IEP_m = k_1(R, m)(b - 1)^{1+k_2(R, m)} IEP^{k_3(R, m)} \quad (22)$$

The coefficients  $k_1$ ,  $k_2$  and  $k_3$  can be evaluated respect to  $R$  and  $m$  by linear interpolation on a board.

Remembering the Eq. 17, and substituting for narrow-band damage the expression:

$$D_{NB} = \frac{v_P T}{k} 2^{\frac{3m}{2}} \Gamma\left(1 + \frac{m}{2}\right) M_0^{\frac{1}{2}} \quad (23)$$

it can be obtained for the corrective coefficient the final relation, where  $\Gamma$  is the well-known gamma function:

$$\lambda = 1 - \frac{1}{2^{\frac{3m}{2}} \Gamma\left(1 + \frac{m}{2}\right) \sqrt{1+R}} IEP_m \quad (24)$$

The observation of Eq. 24 allows to assert that corrective coefficient  $\lambda$  is independent from  $A_1$  and  $k$ , therefore, if slope of Wohler's curve is fixed, it is a function of  $R$  and  $b$ . For example Fig. 15 illustrates its values for  $m = 10$ , that is the standard slope of smooth specimen. Fig. 16 instead for the same bimodal processes of Fig. 14 shows the normalized differences magnitude between  $\lambda_{an}$ , calculated by (24) and  $\lambda_{sim}$ , deriving by time-domain simulation. The highest value of the error is about 4 per cent that is certainly a very good estimate.

The relation contained in (24) is not only a frequency method but also demonstrates that corrective coefficient  $\lambda$  is depending on mechanical system properties and its configuration, while it is not related to the level of the dynamical excitation. In paragraph 5 of this paper it will be shown as this conclusion can be used in a separation of the effects of the determinant factor on the fatigue damage.



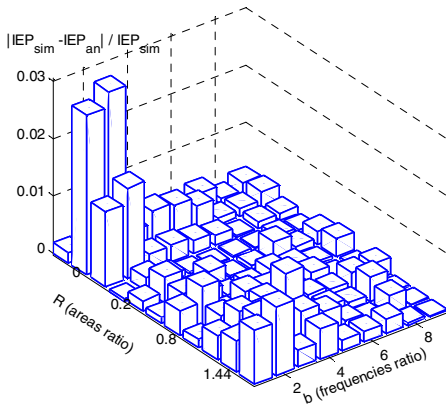


**Figure 14 :** Normalized differences between *IEP* values evaluated in frequency (21) and time domain vs. *b* and *R*

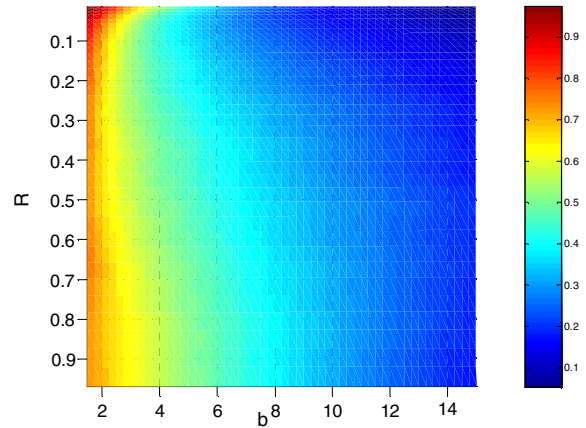


**Figure 15 :** Corrective coefficient  $\lambda$  for  $m = 10$

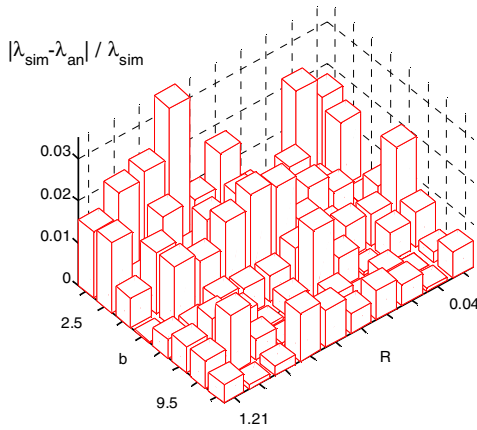


**Figure 16 :** Normalized errors of  $\lambda$  analytical model for  $m = 10$

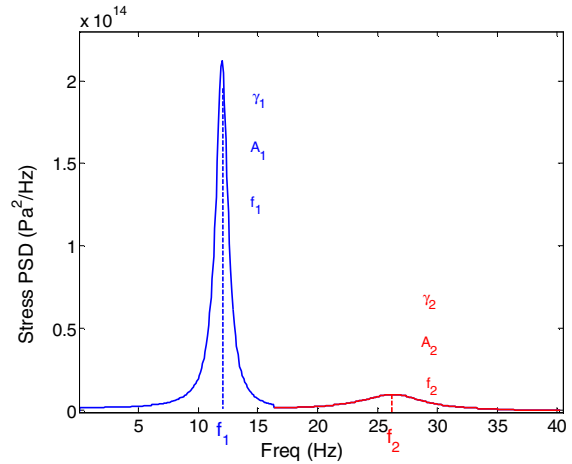


**Figure 17 :** Example of *PSD* formed by linear filters

### 3.4 Numerical simulation

In order to verify the agreement of the analytical model estimates with the time-domain results the authors have performed many set of numerical simulation. In a following section it will be discussed on the extension of the applications field of the proposed method: the results of suitable numerical tests will be shown to support that hypothesis. In this context instead the objective is that of checking the method both starting from other geometrical shape for bimodal *PSD* and on more realistic stress *PSD*.

#### 3.4.1 Other representations of bimodal *PSD*

As previously mentioned triangular shape is not the more frequently used representation in literature. Therefore it

is obvious to wonder if a model optimized by a triangular shape *PSD* works efficiently. A series of time histories with different bandwidth, central frequencies, areas, *R* and *b* has been simulated starting from three shapes of *PSD*: triangular, rectangular and by linear filter. Fig. 17 displays the last of these representations: stress *PSD* is created processing a time signal with uniform frequency spectrum by a linear filter simulating the frequency response of one degree of freedom linear system. The parameters control, more difficult than the others two shapes, is obtained varying damping and stiffness of linear system, in practice by modifying filter coefficients.

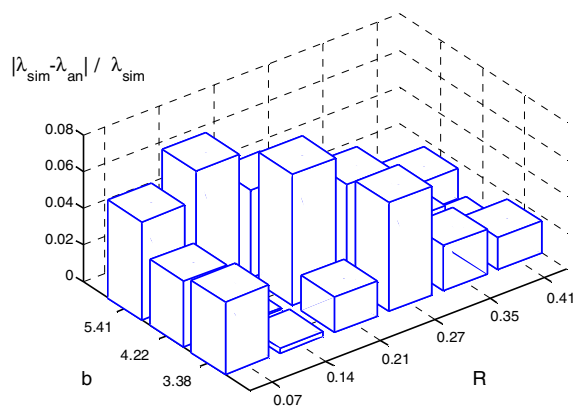
For each process 10 time histories with  $10^5$  fatigue cycles have been reconstructed and the related rainflow results have been averaged to obtain more statistical confidence

**Table 1** : Results of simulation on different shapes of PSD

| set | $f_1$ (Hz) | $A_1$ (Pa2) | $\Delta f$ (%fc) | $b$       | $R$             | Absolute mean error |         |        |
|-----|------------|-------------|------------------|-----------|-----------------|---------------------|---------|--------|
|     |            |             |                  |           |                 | Triang              | Rectang | Filter |
| 1   | 8          | 9e14        | 0.1              | 1.5:0.5:9 | $(0.1:0.1:1)^2$ | 0.0213              | 0.0417  | 0.0221 |
| 2   | 8          | 9e14        | 0.4              | 1.5:0.5:9 | $(0.1:0.1:1)^2$ | 0.0551              | 0.0721  | 0.0491 |
| 3   | 8          | 1.6e15      | 0.1              | 1.5:0.5:9 | $(0.1:0.1:1)^2$ | 0.0331              | 0.0679  | 0.0278 |
| 4   | 8          | 1.6e15      | 0.4              | 1.5:0.5:9 | $(0.1:0.1:1)^2$ | 0.0597              | 0.0821  | 0.0441 |
| 5   | 16         | 9e14        | 0.1              | 1.5:0.5:9 | $(0.1:0.1:1)^2$ | 0.0498              | 0.0712  | 0.0435 |
| 6   | 16         | 9e14        | 0.4              | 1.5:0.5:9 | $(0.1:0.1:1)^2$ | 0.0612              | 0.0931  | 0.0581 |
| 7   | 16         | 1.6e15      | 0.1              | 1.5:0.5:9 | $(0.1:0.1:1)^2$ | 0.0312              | 0.0514  | 0.0327 |
| 8   | 16         | 1.6e15      | 0.4              | 1.5:0.5:9 | $(0.1:0.1:1)^2$ | 0.0665              | 0.0915  | 0.0415 |

for the estimation. Then the derived corrective coefficient has been compared with those evaluated by the Eq. 24. Tab. 1 synthesizes the differences about eight sets of simulated data. Each set is referred to a particular combination of  $f_1$ ,  $A_1$  and bandwidth  $\Delta f$  of unimodal peaks, while  $R$  and  $b$  have been varied into a range with a specified increment. For each set the mean absolute value of the error has been calculated. Observing the table it can be deduced that mean error remains small under all the conditions. It is practically constant for each  $f_1$  and  $A_1$  combination, while only a negligible dependence by  $\Delta f$  has been learned. Moreover PSDs obtained by filter (the more realistic) have the lowest level of error.

### 3.4.2 Finite element beam model

**Figure 18** : Absolute error on finite element beam model

As shown in Fig. 5, exciting a clamped-clamped beam with random input, the normal stress response in its

points will be almost bimodal. The authors have performed some simulations in Matlab® code on a simple dynamic beam model. This is composed by FE beam elements with two degrees of freedom: the vertical displacement (along excitation direction) and the rotation about an axis normal to the plane defined by the beam axis and the excitation direction. By the variations of geometrical (length and normal area) and physical properties (density and Young's modulus) of the model, it has been possible to obtain stress PSD with different frequencies ratio  $b$  and areas ratio  $R$ . Exactly 6 values of  $R$  and 3 of  $b$  have been generated for a total number of 18 bimodal processes. Fig. 18 shows the differences between analytical and simulated corrective coefficient at the same manner of the previous tests. Although the mean error is higher than Fig. 16, also in this situation the proposed analytical model proves to be efficient. Even if the dynamic system of Fig. 5 is very simple, it is a first real example of application for Eq. 24, which seems to recommend its use as frequency method.

## 4 Generalized Bimodal PSD

In real word applications rarely stress PSDs assume such an elementary shape as those presented in the previous sections. In fact dynamical systems of main interest have an high number of degrees of freedom; thus many resonances participate to the frequency response of the component. This theoretically means that the bimodal frequency methods cannot be applied for real state of stress; moreover, as previously explained, random process complexity increases because an equivalent uniaxial PSD generally must be evaluated from more stress components. However, the aspect of the equivalent uniaxial

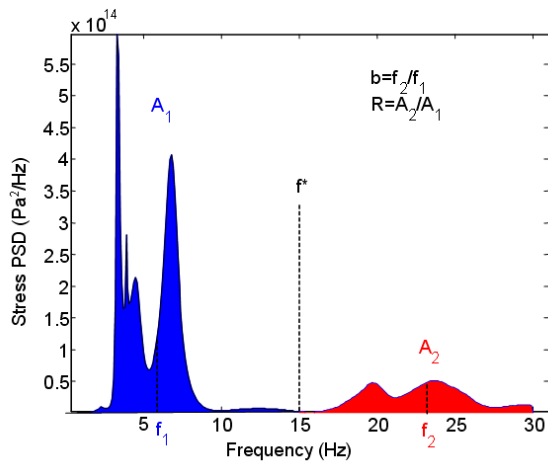


Figure 19 : Generalized Bimodal PSD

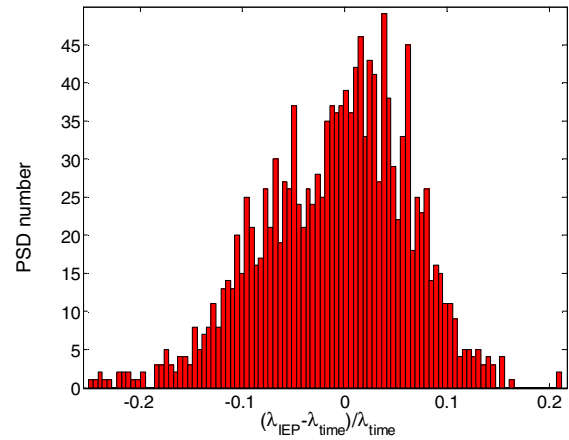


Figure 20 : Histogram of errors on corrective coefficient

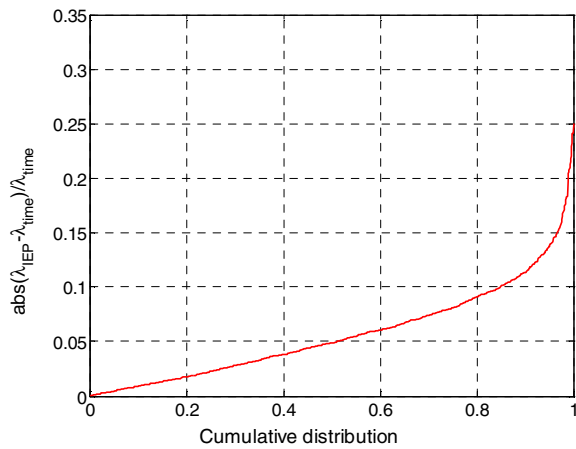


Figure 21 : Cumulative distribution of absolute error

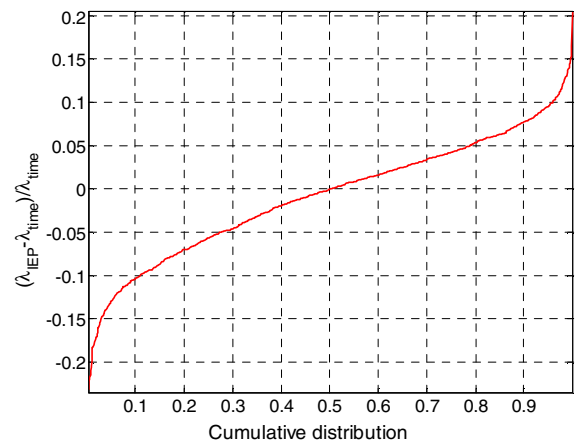


Figure 22 : Cumulative distribution of error with sign

stress frequency representation is very often similar to the one shown in Fig. 19.

Here two zone of spectral area accumulation can be distinguished and the concept of bimodal PSD can be generalized including all the structural responses with two dominant frequencies range. Once the limit  $f^*$  between two zone is defined in proper terms the parameters  $R$  and  $b$  can be estimated simply by Eq. 10 and Eq. 11. Even if there are other processes for which this limit is not easy to characterize, the extension before mentioned allows to employ bimodal frequency method in the greater part of design conditions. It is clear that the validity of this generalization is related to the hypothesis that the fatigue damage depends more from ratio between its accumulation areas central frequencies than the bandwidths of these ones (that is one of the basis of PSD triangular modeling as it was already seen).

To demonstrate the validity of the generalization stated in the former sentences a virtual simulation of a significant test case has been considered from the authors. The data numerically acquired from this test case are a subset of the ones currently used in a “wide range” research conducted by the authors on frequency domain approach for fatigue damage evaluation. The research activity has been presented in the first paragraph of this paper. PSDs of stress random process has been derived on a car chassy by simulating into a MBS environment the full vehicle moving on a pavé at constant velocity. Starting from PSD matrix of the biaxial state of stress (car chassy FE model has been meshed by shell elements and translated into a modal model using Craig and Bampton approach) an equivalent uniaxial PSD has been evaluated for each element. Fig. 19 is an example of these random processes. By the application of the theory about IEP method it can

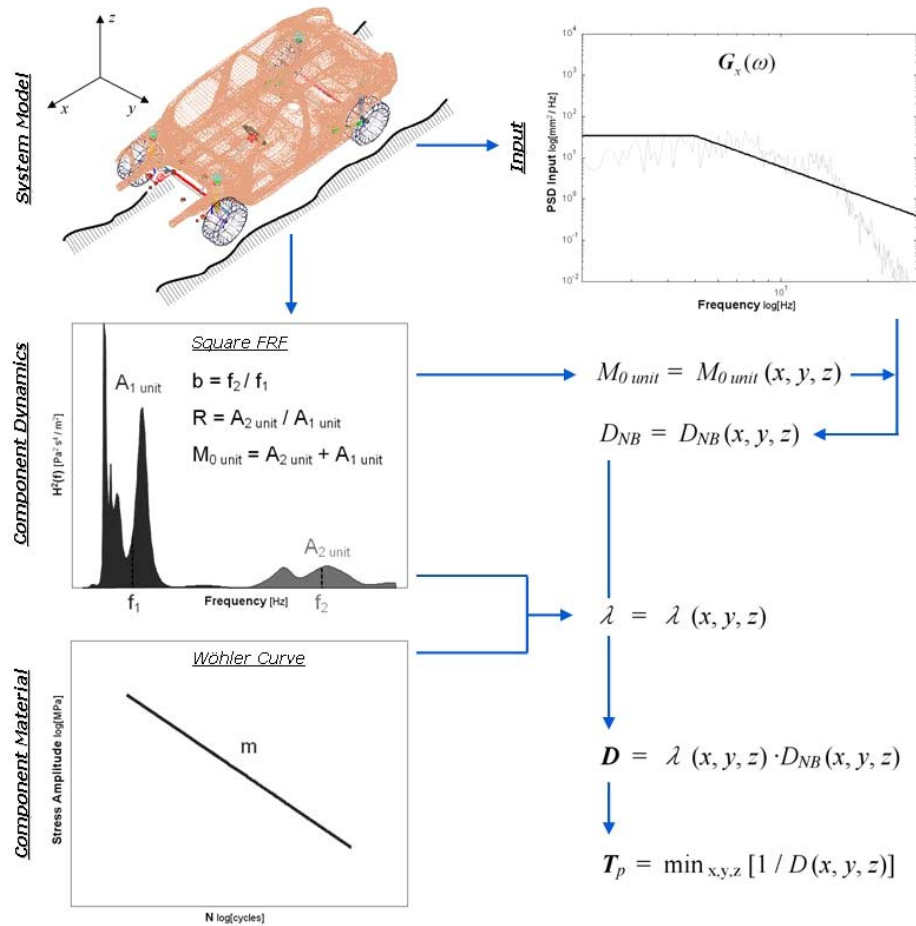


Figure 23 : Proposed method flow chart

be evaluated the corrective coefficient  $\lambda$  for each of selected elements (in number of approximately 1600). This estimation of  $\lambda$  has been compared with the same coefficient evaluated by Rainflow Counting as already seen for the other tests. Fig. 20 shows an histogram of the differences found. The definition of transition frequency  $f^*$  has been carried out by minimizing *PSD* function in the interval of frequencies [10 Hz, 20 Hz]. This definition is certainly arbitrary and it must be improved out. Of the 1600 elements about 50 (3 per cent) has been discarded because it has not been possible to define the limit  $f^*$ .

It is also possible to verify the goodness of the results looking at Fig. 21 and Fig. 22. Fig. 21 shows cumulative distribution of absolute error of *IEP* method, while Fig. 22 represents cumulative distribution of error with sign on all the elements. Only the 15 per cent of the estimations exceeds the absolute error of 0.1 and about the 3 per cent exceed the absolute value of 0.15.

It can be appreciated also that the mean value of the error with sign is substantially zero. This fact is important because it denotes an unbiased method. Moreover, on the cumulative distribution a problem of damage statistical convergence is implicit: an average value of damage on 10 time histories containing  $10^5$  fatigue cycles has been calculated for each process. This estimation has a good degree of confidence, but certainly it is far from full convergence. Then the mean absolute error represented in Fig. 21 is higher than the true mean absolute error.

In conclusion, the *IEP* method supply good agreement to the time-domain approach for generalized bimodal shape of *PSD* too.

### 5 Why a new frequency method?

In the last years many researchers has been involved in the study of an efficient frequency method for fatigue damage estimation under wide band stress conditions.

However they usually process many stress time histories but they don't care how these stresses are generated into the mechanical system. Instead one objective of this paper has been related to the dependence of corrective coefficient  $\lambda$  on the dynamical local properties of the system. Fig. 23 shows this aspect for a car chassis: as previously demonstrated, the corrective coefficient of the narrow-band formula  $\lambda$  is a function only of  $R$ ,  $b$  and  $m$ . Therefore it can be seen as a local property of mechanical system under a particular configuration, not depending by the level of the input (if input is constant on the frequency range of interest, as usually it is modeled). The  $R$  and  $b$  values can be found starting from the knowledge of frequency response for all elements. A frequency analysis with unitary level of input  $PSD$  is a simple way to obtain squared frequency responses. Then the damage evaluated with the narrow-band formula will change varying the input level, but corrective coefficient will not change and it is known for all input conditions (provided it is constant on the frequencies of interest). Therefore the fatigue damage of bimodal  $PSD$  (in classic sense or in generalized definition) can be successfully reduced to an analytical problem depending on four variables: the slope of material Wohler's curve, that is related to the fatigue behaviour, the stress  $PSD$  ratios  $b$  and  $R$ , which reproduce the local dynamic properties of the system and the values  $A_1$ , that is strictly connected with the level of the input. The development of a more elegant analytical relation for  $\lambda$  will be a future objective of the authors, but the aim of a complete problem understanding seems to be successfully achieved.

## 6 Conclusions and future objectives

One of the future aims will consist in a more compact formulation of the  $\lambda$  analytical model as it has been previously explained. Some functions may be optimized and other relations must be completed, as the order  $m$   $IEP$  dependence by  $m$  and  $R$ , which has been only partially made explicit. Moreover other parameters ( $\gamma_1$  and  $\gamma_2$  for example) can be included in the analytical model. However this is a secondary requirement because the authors are interested to an efficient use of the frequency approach to fatigue evaluation and the results reached by the present model are already suitable to this aim. In fact in this paper some numerical simulation have been used to demonstrate the efficiency of  $IEP$  method, by comparison with time histories reconstructed both from bi-

modal  $PSDs$  of elementary shape and from  $PSDs$  derived by a frequency analysis on a  $FEM$  model of a car body. Furthermore a physical interpretation of the relations between  $\lambda$  and the variables chosen for the analytical model has been supplied. Obviously the authors also want to make a careful study on this interpretation in future activities of research.

## References

- Bendat J. S.** (1964): Probability functions for random responses. In: NASA report on contract NAS-5-4590
- Bishop, N. W. M.; Sherratt, F.** (1990): A theoretical solution for the estimation of Rainflow ranges from Power Spectral Density data. In: Fatigue Fracture Engineering Materials Structures, vol.13.
- Bishop, N. W. M.** (1988): The use of frequency domain parameters to predict structural fatigue, Ph. D. Thesis, University of Warwick.
- Braccesi, C.; Cianetti, F.** (2004): Development of selection methodologies and procedures of the modal set for the generation of flexible body models for multibody simulations. In: Proceedings of the Institution of Mechanical Engineers Part K-Journal of Multi-Body Dynamics, Vol.218, pp.19-30
- Braccesi, C.; Cianetti, F.; Lori G.; Pioli D.** (2004): Sviluppo di una metodologia alternativa per la valutazione virtuale del comportamento a fatica di componenti meccanici soggetti a sollecitazioni di tipo random. In: Proceedings of XXXIII Convegno Nazionale AIAS, Bari, Italy.
- Braccesi, C.; Cianetti, F.; Landi L.** (2005): Random loads fatigue. The use of spectral methods within multibody simulation. In: Proceedings of IDET/CIE ASME 2005, 20<sup>th</sup> Biennial Conference on Mechanical Vibration and Noise, Long Beach (CA), 24-28 September 2005
- Braccesi, C.; Cianetti, F.** (2005): A procedure for the virtual evaluation of the stress state of mechanical systems and components for automotive industry: development and experimental validation. In: Proceedings of the Institution of Mechanical Engineers Part D-Journal of Automobile Engineering, Vol.219, pp.633-643
- Braccesi, C.; Cianetti, F.; Lori G.; Pioli, D.** (2005): L'approccio nel dominio della frequenza alla valutazione del comportamento a fatica di componenti meccanici soggetti a sollecitazioni di tipo random. In: Proceedings

of Giornata di studio sulla Progettazione a fatica in presenza di multiassialità tensionali, Ferrara, Italy.

**Braccesi, C.; Cianetti, F.; Lori G.; Pioli, D.** (2005): Fatigue behaviour analysis of mechanical components subjected to random bimodal stress process: frequency domain approach. In: International Journal of Fatigue, vol. 27, pp. 335-345.

**Kihl, D. P.; Sarkani S.; Beach J. E.** (1995): Stochastic fatigue damage accumulation under broadband loadings. In: International Journal of Fatigue, vol. 17, n.5, pp.321-329

**Lutes L.D** (1990): An improved spectral method for variable amplitude fatigue prediction. In: Journal of the Structural Division, ASCE, vol.116, pp 1149-1164

**Lutes, L. D.; Sarkani S.** (1997): Stochastic analysis of structural and mechanical vibrations. Prentice Hall.

**Matsuishi, M.; Endo, T.** (1968): Fatigue of metals subjected to varying stress. In: Japan Society of Mechanical Engineers, Fukuoka, Japan.

**Papadopoulos, I. V.; Davoli, P.; Gorla, C. ; Filippini M.; Bernasconi, A.** (1997): A comparative study of multiaxial high cycle fatigue criteria for metals. In: International Journal of Fatigue, vol. 19, n.3, pp.219-235

**Pitoiset, X.; Rychlik, I.; Preumont, A.** (2001): Spectral methods to estimate local multiaxial fatigue failure for structures undergoing random vibrations. In: Blackwell Science Ltd, Fatigue Fracture Engineering Material Structures, vol.24, pp. 715-727.

**Rice, J. R.; Beer F.P.** (1965): On the distribution of rises and falls in a continuous random process. In: ASME Basic Engineering, 87, pp. 398-404.

**Vanmarke, E. H.** (1972): Properties of spectral moments with applications to random vibrations. In: Journal Engineering Mechanical Division, ASCE, 98 (2), pp. 425-446.

**Wirsching P. H.; Light, M. C.** (1980): Fatigue under wide-band random stresses. In: Journal of the Structural Division, ASCE, vol.106, pp.1593-1607

**You, B. R.; Lee, S. B.** (1996): A critical review on multiaxial fatigue assessments of metals. In: International Journal of Fatigue, vol. 18, n.4, pp.235-244